processes

MDPI

Communication

Structural Optimization of Alkylbenzenes as Graphene Dispersants

Shimpei Takeda [1] and Yuta Nishina [1,2,*]

[1] Graduate School of Natural Science & Technology, Okayama University; Okayama 700-8530, Japan; p3bq9uip@s.okayama-u.ac.jp
[2] Research Core for Interdisciplinary Sciences, Okayama University; Okayama 700-8530, Japan
* Correspondence: nisina-y@cc.okayama-u.ac.jp

Received: 21 January 2020; Accepted: 12 February 2020; Published: 19 February 2020

Abstract: Among the several methods of producing graphene, the liquid-phase exfoliation of graphite is attractive because of a simple and easy procedure, being expected for mass production. The dispersibility of graphene can be improved by adding a dispersant molecule that interacts with graphene, but the appropriate molecular design has not been proposed. In this study, we focused on aromatic compounds with alkyl chains as dispersing agents. We synthesized a series of alkyl aromatic compounds and evaluated their performance as a dispersant for graphene. The results suggest that the alkyl chain length and solubility in the solvent play a vital role in graphene dispersion.

Keywords: graphene; graphite; dispersant; alkylbenzene; liquid-phase exfoliation

1. Introduction

Graphene, a two-dimensional material composed of honeycomb-shaped sp^2 carbons, was isolated in 2004 [1]. Due to its excellent properties, such as electrical conductivity [2], thermal conductivity [3], and mechanical strength [4], graphene has attracted significant attention. Various applications, such as sensors [5], batteries [6], inks [7], transparent electrodes [8], and others have been extensively investigated. Preparation methods of graphene are roughly divided into two types. One is the bottom-up approach, such as chemical vapor deposition and organic synthesis methods that correspond to assembling atoms or molecules. Chemical vapor deposition can produce large-area graphene, but the method requires expensive substrates, high temperatures, and low pressures [9], making the process less cost-effective. The other is a top-down approach, which includes mechanical exfoliation and oxidative exfoliation, followed by reduction, and ultrasonic exfoliation. The mechanical exfoliation of graphite with scotch tape is quite simple, and high-quality graphene can be obtained. However, the size of the obtained graphene is small (several μm) and cannot be controlled; therefore, mechanical exfoliation is not suitable for the industrial-scale production of graphene [10]. The oxidative-reduction method is capable of synthesizing graphene in large quantities with high yield, but the need for harmful oxidant, and the formation of defects during the processes are problems that have yet to be solved [11–14]. Ultrasonic irradiation is attractive among these methods because it does not require any harmful chemicals and provides relatively high-quality graphene as dispersion [15–17]. In this method, graphite is exfoliated to graphene by irradiating ultrasonic in a solvent, and then graphene dispersion can be obtained. Previous studies have shown that N-methylpyrrolidone (NMP) or dimethylformamide (DMF), which have similar surface energies to graphene, are suitable solvents [18]. However, the use of these solvents has not yet met the requirements for practical application; for example, the concentration of graphene is generally low. In order to improve the concentration of graphene in a solvent, adding molecules that interact with graphene has been investigated, which enabled graphene to be dispersed in a high concentration, even in solvents other than NMP and DMF [19,20]. A guideline for designing

a molecule that can act as a dispersant is as follows; the interaction between the molecule and graphene is stronger than that between the solvent and graphene [21]. Previously, Samori et al. reported that octylbenzene can disperse graphene efficiently, despite its simple structure [22]. Octylbenzene is a type of alkylbenzene; however, in their research, other molecules were not investigated. It has been under the argument that the alkyl chain [23–27] or aromatic moiety [28–36] contributes to the graphene dispersion. To make clear the role of the alkyl chain and the aromatic moiety of the dispersant, we synthesized a series of alkylbenzenes and evaluated their graphene dispersing abilities. Butylbenzene, octylbenzene, and hexadecylbenzene were prepared to compare the effect of the length of the alkyl chain for graphene dispersion. Besides, octylnaphthalene and octylphenanthrene were prepared as dispersants having different aromatic ring structures. 1,4-Dioctylbenzene and 1,3,5-trioctylbenzene were prepared to compare the effect of the number of alkyl chains. Using these molecules, we optimized alkyl chains, aromatic rings, and the number of alkyl chains on a graphene dispersant. Finally, we analyzed the morphology of graphene obtained by using the best dispersant in our research. Our results will contribute to designing and creating new molecules with a high graphene dispersing ability for the mass production of graphene.

2. Materials and Methods

2.1. Materials

Natural flake graphite (Z5F) was purchased from Ito graphite Co. ltd. (Mie, Japan) NMP was purchased from Wako Pure Chemical Industries, Ltd. (Osaka, Japan), then used without further purification. Butylbenzene, octylbenzene, hexadecylbenzene, octylnaphthalene, octylphenanthrene, 1,4-dioctylbenzene, and 1,3,5-trioctylbenzene were synthesized following the reported procedures [37,38]. Details are described in the supporting information.

A laser Raman spectrophotometer (NRS-5100NPS manufactured by JASCO Corporation, Tokyo, Japan) was used to compare graphite and exfoliated graphene, and to examine the defect density of dispersed graphene. Raman scattering was carried out using a single monochromator with a diode-pumped single-frequency laser and a Peltier cooled Charge Coupled Device (CCD) camera (NRS5100 manufactured by JASCO Corporation, Tokyo, Japan). Wavelength and power of the laser were 532 nm and 5.7 mW, respectively. The polarized incident beam was focused onto the sample's surface by the objective lens (×100). The spectral resolution was 1.8 cm^{-1}. A scanning electron microscope (s-5200, manufactured by Hitachi High-Technologies Corporation, Tokyo, Japan) was used to measure the size of the flakes of graphite and exfoliated graphene. Samples were prepared by adding 5 μL of as-prepared graphene dispersion and 1 mL of chloroform to a microtube, mildly irradiating ultrasonic waves to homogenize the dispersion, dropping it on a Si substrate, and vacuum-drying at 50 °C for 1 day before SEM measurement. The measurements were made under a voltage of 20 kV. A scanning probe microscope (SPM-9700, manufactured by Shimadzu Corporation, Kyoto, Japan) was used to measure the size and thickness of the exfoliated graphene. The sample was prepared by adding 10 μL of the as-prepared graphene dispersion and 1 mL of chloroform to a microtube, mildly irradiating ultrasonic waves to homogenize the dispersion, dropping it on a mica substrate, and drying at 50 °C for 1 day under vacuum. Atomic Force Microscope (AFM) measurement was performed in dynamic mode using 10 μm cantilever.

The structure of molecules was determined by ^{1}H nuclear magnetic resonance (^{1}H-NMR) using a Varian NMR System 400 MHz using $CDCl_3$ as a solvent.

2.2. Exfoliation of Graphite and Evaluation of Graphene Dispersion

The dispersing conditions were determined following the previous report [22]; the dispersing agent was added to the solvent so that the volume ratio became 15% (dispersing agent 1.5 mL, NMP 8.5 mL), and 100 mg of graphite was added. Using an ultrasonic irradiation device (BILON150-Y, manufactured by Shanghai Bilon Instrument Co., Ltd, Shanghai, China) with an output of 250 W, pulse:

irradiation 1 s/stop 1 s. The sonication was performed while cooling with ice water for 6 h. Thereafter, in order to remove non-exfoliated graphite, centrifugation was performed at 6000 rpm for 30 min (LC-200 manufactured by Tomy Seiko Co., Ltd., Tokyo, Japan), and the supernatant (3 mL) was taken as a graphene dispersion. The concentration of graphene was determined by UV-Vis spectroscopy (V750 manufactured by JASCO Corporation, Tokyo, Japan) using a glass cell, which is shown in the supporting information.

2.3. Recovery and Reuse of Dispersants

The graphene dispersion prepared with 1,4-dioctylbenzene as dispersant was vacuum-filtered, and washed with water and hexane to remove NMP and the dispersant from graphene. The organic phase was dried over magnesium sulfate and the solvent was removed in vacuo. The recovered compound was analyzed by ^{1}H NMR (Figure S5).

3. Results and Discussion

3.1. Evaluation of Graphene Dispersant

Initially, the exfoliation of graphite was performed without using any dispersant in NMP to give 22 μg/mL graphene dispersion (Table 1, Entry 1). Octylbenzene, which was reported previously [22], provided a graphene dispersion of 101 μg/mL (Table 1, Entry 2). When a shorter and longer alkyl chain was introduced in the dispersant structure, a graphene dispersion of 92 μg/mL and 128 μg/mL were obtained, respectively (Table 1, Entries 3 and 4). These results suggest that the longer alkyl chain is more efficiently exfoliate graphite and disperse graphene in the solvent. A similar result was reported using carboxylic acids as dispersants; as a result, the concentration of graphene increased as the number of carbon atoms in the carboxylic acid increased to 30 [23]. However, in our research, when the graphene dispersion using hexadecylbenzene was allowed to stand for several days, phase separation and aggregation of graphene was observed (Figure S4). The reason for this phenomenon would be that the dispersant molecule with a long alkyl chain and aromatic ring was hardly dissolved in the solvent (NMP). Then, graphene moved to the dispersant phase that strongly interacts with the graphene. Such phase separation may be caused by the lower affinity of the benzene ring for the solvent, because alkyl carboxylic acid did not show such separation [23].

Next, graphite was subjected to liquid-phase exfoliation using aromatic compounds with different numbers of aromatic rings. Octylnaphtharene and octylphenanthrene produced a graphene dispersion of 35 μg/mL and 10 μg/mL, respectively (Table 1, Entries 5 and 6). Aromatic compounds have been used as dispersants for graphene, because they have strong affinity through π–π interaction. In fact, many dispersants having a pyrene or perylene structure have been reported [28,35], and it was expected that the larger the aromatic ring, the stronger the interaction with graphene, and the better the dispersibility will be obtained. However, in our system, aromatic rings did not contribute to the dispersion. As the number of aromatic rings increased, the dispersibility decreased, and when octylphenanthrene was used (Table 1, Entry 6), the dispersibility was lower than without dispersant (Table 1, Entry 1). This result suggests that—not only the interaction between graphene and the dispersant—but also the affinity between the solvent and the dispersant is important for the dispersion of graphene. Based on this assumption, we expected that the degree of dispersion could be improved by introducing multiple alkyl chains to one aromatic ring. To confirm the effect of the number of alkyl chains, 1,4-dioctylbenzene and 1,3,5-trioctylbenzene were synthesized as dispersants, and their performance for graphene dispersion was evaluated. When 1,4-dioctylbenzene was used, 306 μg/mL graphene dispersion was obtained (Table 1, Entry 6). This value was about three times higher than that of octylbenzene. The 1,3,5-trioctylbenzene was expected to work as a better dispersant, but it was not dissolved in NMP, and we could not evaluate its performance (Table 1, Entry 7). From the above results, the longer and larger numbers of alkyl chains are more suitable for graphene dispersion; the interaction with solvents should also be considered. On the other hand, the aromatic ring does not

need to be large, and a benzene ring is sufficient. In other words, to get better graphene dispersion, the balance between the length and numbers of the alkyl chain and the size of the aromatic ring need to be optimized.

Table 1. Relationship between dispersant structure and the concentration of grapheme [a].

Entry	Dispersant		Concentration of Graphene
1	None		22 μg/mL
2	Octylbenzene	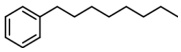	92 μg/mL
3	Butylbenzene	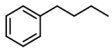	101 μg/mL
4	Hexadecylbenzene	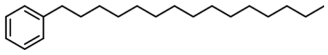	(128 μg/mL) [b]
5	Octylnaphthalene	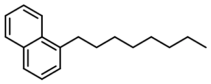	35 μg/mL
6	Octylphenanthrene	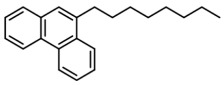	10 μg/mL
7	1,4-Dioctylbenzene	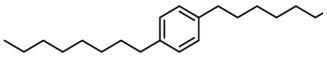	306 μg/mL
8	1,3,5-Trioctylbenzene	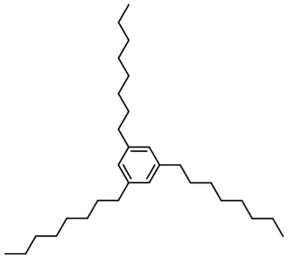	- [c]

[a] Graphite (100 mg), dispersant (1.5 mL), and N-methylpyrrolidone (NMP) (8.5 mL) was mixed and sonicated for 6 h. Then the mixture was centrifuged (6000 rpm for 30 min). [b] Phase separation occurred after several days. [c] The dispersant was not dissolved in the solvent.

3.2. Structure and Morphology Analysis

We then characterized graphene exfoliated with 1,4-dioctylbenzene, which is the most effective dispersant. Graphene exfoliated with octylbenzene, which is a reported dispersant, was used for comparison. Initially, size analysis was performed by using electron scanning microscopy (SEM). The graphite before exfoliation had a size distribution of about 2 to 5 μm, and stacked morphology (Figure S1). Graphene sheets of several tens of nm were observed when octylbenzene or 1,4-dioctylbenzene was used as a dispersant (Figure 1a,b). The reduction of the flake size may be caused by the sonication process, cleaving the carbon frameworks. Since there was no significant difference in the flake size between 1,4-dioctylbenzene and octylbenzene, the graphene sheet size was hardly affected by the alkyl chain of the dispersant. This result is conflicting, to when graphite was dispersed in water using dispersants having different alkyl chains, in which a longer alkyl chain resulted in larger sized graphene [25]. The reason for the contradiction between our result and the previous report is unclear at this moment. Still, we consider that the dispersion and stabilization mechanism is different when different solvents and different dispersant structures are employed. Next, the atomic force microscope (AFM) measurement was performed to understand the thickness and size of the exfoliated graphene. Graphene obtained using octylbenzene and 1,4-dioctylbenzene both had a size of about 100 nm and a thickness of about 1 nm (Figure 1c,d). As in the results of the SEM measurements, graphene sheets with similar size distributions were observed, regardless of the structure of the dispersant. Considering the thickness of single-layer graphene is 0.335 nm [39], and the dispersants are attached on the graphene surface, our graphene sheets are 1–2 layers. Based on the

morphological analysis by SEM and AFM, the dispersant designed with different alkyl chains, such as octylbenzene and 1,4-dioctylbenzene, did not affect the size and thickness of graphene.

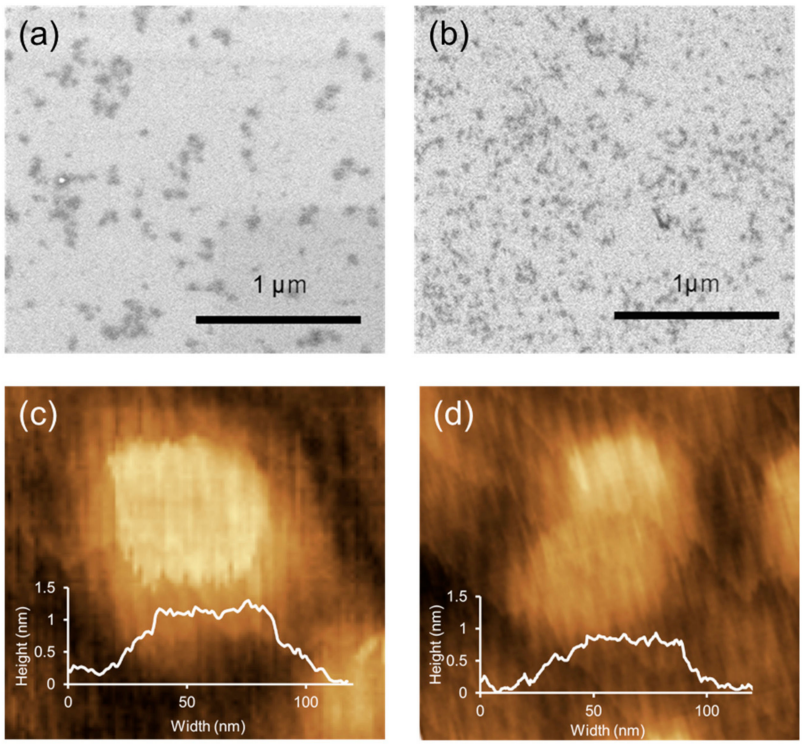

Figure 1. SEM images of graphene dispersed by (**a**) octylbenzene and (**b**) 1,4-dioctylbenzene, and AFM images of graphene dispersed by (**c**) octylbenzene and (**d**) 1,4-dioctylbenzene.

Raman spectra were measured to examine defects of graphene. Compared to graphite before exfoliation, graphene sheets obtained with octylbenzene and 1.4-dioctylbenzene showed a stronger D band. The D band was attributed to the defect structure and edge of graphene [40], and the ratio of the D band to G band, I_D/I_G, was 0.33 for graphite before exfoliation. The I_D/I_G values of octylbenzene-derived graphene and 1,4-dioctylbenzene-derived graphene were 1.13 and 1.26, respectively (Figure 2). The D bands were derived from edges and holes (defects) formed during the cleaving process. Since the size of graphene obtained from octylbenzene and 1,4-dioctylbenzene was almost the same, the effect of edges for the D band should be the same. Nevertheless, 1,4-dioctylbenzene had a larger D band, indicating that this dispersant created more defects in the basal plane of graphene. The 2D band is related to the disorder of the graphene structure [40]. Graphite with many graphene layers has an asymmetric peak; in contrast, the graphene with fewer layers shows a symmetric and sharp peak [40]. The 2D band of graphite before exfoliation was asymmetric, whereas the graphene obtained using octylbenzene and 1,4-dioctylbenzene showed symmetric 2D bands. In addition, a shoulder-like peak (D′ band) appears at a position close to the G band of graphene [41]. In our Raman measurements, no D′ band was found in graphite, but observed in exfoliated graphene. This also proved that the graphene sheets obtained using the alkylbenzene dispersants are sufficiently exfoliated.

3.3. Recovery and Reuse of Dispersants

The graphene dispersion was filtered to separate graphene from solvent and dispersant. The filtered graphene film was washed with hexane to remove residual dispersant. As a result, 97% of the used dispersant was recovered. Besides, structural analysis by ^{1}H NMR of the recovered dispersant showed that no structural change by the dispersing and separation procedures (Figure S5). Some of the reported dispersants interact strongly with graphene and can remain on its surface [21], affecting

the properties of the graphene. The 1,4-dioctylbenzebe developed in this study can disperse graphene at a high concentration, while it can easily be removed from graphene, enabling recovery and reuse.

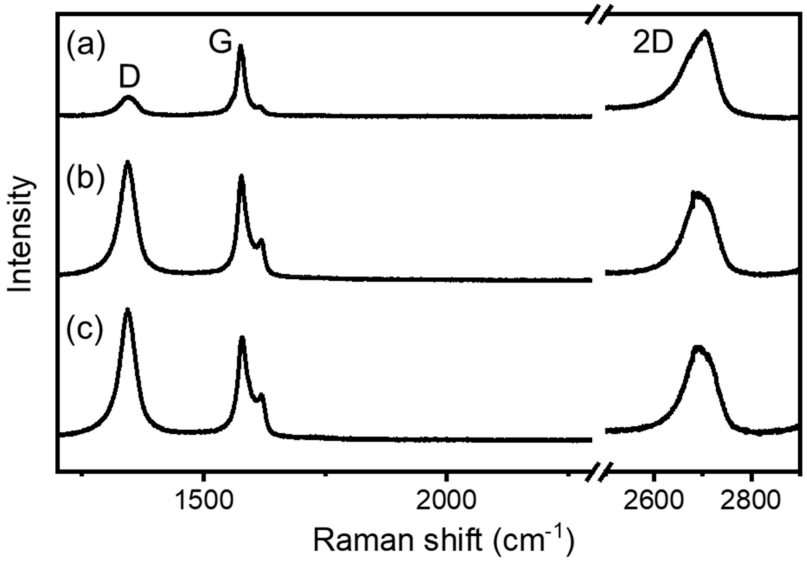

Figure 2. Raman spectra of (**a**) graphite and graphene dispersed by (**b**) octylbenzene and (**c**) 1,4-dioctylbenzene.

4. Conclusions

In this study, we examined how the structure of the dispersant affected the dispersibility of graphene and succeeded in establishing a guideline for creating a new high-performance dispersant. The 1,4-dioctylbenzene resulted in a graphene dispersion at a concentration three times higher than that of a conventional alkylbenzene dispersant. It was found that the performance of the graphene dispersant greatly depended on the structures of the alkyl chain and the aromatic ring. Namely, as the length and the number of alkyl chains in the dispersing agent increased, the dispersibility of graphene increased. However, if the length and number are too large, the dispersing agent became insoluble in the solvent, then it could not work. In other words, when designing a dispersant, it is necessary to consider not only the interaction with graphene but also the affinity for a solvent, and precise molecular design is required. As a result of evaluating the size and thickness of the exfoliated graphene by SEM and AFM, it was found that graphite was exfoliated into one or two layers of graphene. Graphene size hardly changed, irrespective of the length of the alkyl chain of the dispersant. On the other hand, graphene obtained by using a dispersant with high dispersibility (1,4-dioctylbenzene) showed larger amounts of defects, determined by Raman analysis.

The dispersant was not decomposed under graphite exfoliation procedures, could be easily extracted from graphene using hexane, and could be recovered in a high recovery rate. This means that the graphene prepared by this method did not contain a dispersant, and may solve the problem of the contamination of the dispersant, which has been a problem in the conventional graphene dispersion. The graphene obtained in this study still has many defects and small size. The development of a graphene dispersant that solves these problems is strongly required. Based on the findings obtained in this study, we want to produce high-quality graphene and apply it to electronic devices.

Supplementary Materials: The following are available online at http://www.mdpi.com/2227-9717/8/2/238/s1, Figure S1: SEM image of natural flake graphite used in this research, Figure S2: UV-Vis spectra of 5 different concentrations of graphene dispersion, Figure S3: Calibration curve of absorbance of graphene at 800 nm, Figure S4: Dispersion using hexadecylbenzene immediately after sonication (left) and several days after (right), Figure S5: ^{1}H NMR spectrum of 1,4-dioctylbenzene after recovery.

Author Contributions: Conceptualization, Y.N.; experiment, S.T.; writing—original draft preparation, S.T.; writing—review and editing, Y.N.; funding acquisition, Y.N. All authors have read and agreed to the published version of the manuscript.

Funding: This research was funded by JST A-STEP, grant number 19-191030677.

Conflicts of Interest: The authors declare no conflict of interest. The funders had no role in the design of the study; in the collection, analyses, or interpretation of data; in the writing of the manuscript, or in the decision to publish the results.

References

1. Novoselov, K.S.; Geim, A.K.; Morozov, S.V.; Jiang, D.; Zhang, Y.; Dubonos, S.V.; Grigorieva, I.V.; Firsov, A.A. Electric Field Effect in Atomically Thin Carbon Films. *Science* **2004**, *306*, 666–669. [CrossRef]
2. Mayorov, A.S.; Gorbachev, R.V.; Morozov, S.V.; Britnell, L.; Jalil, R.; Ponomarenko, L.A.; Blake, P.; Novoselov, K.S.; Watanabe, K.; Taniguchi, T.; et al. Micrometer-scale ballistic transport in encapsulated graphene at room temperature. *Nano. Lett.* **2011**, *11*, 2396–2399. [CrossRef] [PubMed]
3. Balandin, A.A. Thermal properties of graphene and nanostructured carbon materials. *Nat. Mater.* **2011**, *10*, 569–581. [CrossRef]
4. Yang, Z.; Gao, R.; Hu, N.; Chai, J.; Cheng, Y.; Zhang, L.; Wei, H.; Kong, E.S.; Zhang, Y. The Prospective Two-Dimensional Graphene Nanosheets: Preparation, Functionalization and Applications. *Nano-Micro. Lett.* **2012**, *4*, 1–9. [CrossRef]
5. Bae, S.; Lee, Y.; Sharma, B.K.; Lee, H.; Kim, J.; Ahn, J. Graphene-based transparent strain sensor. *Carbon* **2013**, *51*, 236–242.
6. Reddy, A.L.M.; Srivastava, A.; Gowda, S.R.; Gullapalli, H.; Dubey, M.; Ajayan, P.M. Synthesis of nitrogen-doped graphene films for lithium battery application. *ACS Nano.* **2010**, *4*, 6337–6342. [CrossRef] [PubMed]
7. Shboul, A.A.; Trudeau, C.; Cloutier, S.; Siaj, M.; Claverie, J.P. Graphene dispersions in alkanes: Toward fast drying conducting inks. *Nanoscale* **2017**, *9*, 9893–9901. [CrossRef] [PubMed]
8. Li, X.; Zhu, Y.; Cai, W.; Borysiak, M.; Han, B.; Chen, D.; Piner, R.D.; Colombo, L.; Ruoff, R.S. Transfer of Large-Area Graphene Films for High-Performance Transparent Conductive Electrodes. *Nano Lett.* **2009**, *9*, 4359–4363. [CrossRef]
9. Li, X.; Cai, W.; An, J.; Kim, S.; Nah, J.; Yang, D.; Piner Velamakanni, A.; Jung, I.; Tutuc, E.; Banerjee, S.K.; et al. Large-area synthesis of high-quality and uniform graphene films on copper foils. *Science* **2009**, *324*, 1312–1314. [CrossRef]
10. Geim, A.K.; Novoselov, K.S. The rise of graphene. *Nat. Mater.* **2007**, *6*, 183–191. [CrossRef]
11. Hu, Y.; Song, S.; Lopez-Valdivieso, A. Effects of oxidation on the defect of reduced graphene oxides in graphene preparation. *J. Colloid. Interface Sci.* **2015**, *450*, 68–73. [CrossRef]
12. Johnson, D.W.; Dobson, B.P.; Coleman, K.S. A manufacturing perspective on graphene dispersions. *Curr. Opin. Colloid Interface Sci.* **2015**, *20*, 367–382. [CrossRef]
13. Konios, D.; Stylianakis, M.M.; Stratakis, E.; Kymakis, E. Dispersion behaviour of graphene oxide and reduced graphene oxide. *J. Colloid Interface Sci.* **2014**, *430*, 108–112. [CrossRef] [PubMed]
14. Price, E.K.; Bansala, T.; Achee, T.C.; Sun, W.; Green, M.J. Tunable dispersibility and wettability of graphene oxide through one-pot functionalization and reduction. *J. Colloid Interface Sci.* **2019**, *552*, 771–780. [CrossRef] [PubMed]
15. Guardia, L.; Fernández-Merino, M.J.; Paredes, J.I.; Solís-Fernández, P.; Villar-Rodil, S.; Martínez-Alonso, A.; Tascón, J.M.D. High-throughput production of pristine graphene in an aqueous dispersion assisted by non-ionic surfactants. *Carbon* **2011**, *49*, 1653–1662. [CrossRef]
16. Khan, U.; O'Neill, A.; Porwal, H.; May, P.; Nawaz, K.; Coleman, J.N. Size selection of dispersed, exfoliated graphene flakes by controlled centrifugation. *Carbon* **2012**, *50*, 470–475. [CrossRef]
17. Alaferdov, A.V.; Gholamipour-Shirazi, A.; Canesqui, M.A.; Danilov, Y.A.; Moshkalev, S.A. Size-controlled synthesis of graphite nanoflakes and multi-layer graphene by liquid phase exfoliation of natural graphite. *Carbon* **2014**, *69*, 525–535. [CrossRef]

18. Hernandez, Y.; Nicolosi, V.; Lotya, M.; Blighe, F.M.; Sun, Z.; De, S.; Holland, B.; Byrne, M.; Gun, Y.; Boland, J.; et al. High-yield production of graphene by liquid-phase exfoliation of graphite. *Nat. Nanotechnol.* **2008**, *3*, 563–568. [CrossRef]
19. Lotya, M.; Hernandez, Y.; King, P.J.; Smith, R.J.; Nicolosi, V.; Karlsson, L.S.; Blighe, F.M.; De, S.; Wang, Z.; McGovern, I.T.; et al. Liquid phase production of graphene by exfoliation of graphite in surfactant/water solutions. *J. Am. Chem. Soc.* **2009**, *131*, 3611–3620. [CrossRef]
20. Xu, L.; McGraw, J.W.; Gao, F.; Grundy, M.; Ye, Z.; Gu, Z.; Shepherd, J.L. Production of High-Concentration Graphene Dispersions in Low-Boiling-Point Organic Solvents by Liquid-Phase Noncovalent Exfoliation of Graphite with a Hyperbranched Polyethylene and Formation of Graphene/Ethylene Copolymer Composites. *J. Phys. Chem. C* **2013**, *117*, 10730–10742. [CrossRef]
21. Ciesielski, A.; Samorì, P. Supramolecular Approaches to Graphene: From Self-Assembly to Molecule-Assisted Liquid-Phase Exfoliation. *Adv. Mater.* **2016**, *28*, 6030–6051. [CrossRef]
22. Haar, S.; El Gemayel, M.; Shin, Y.; Melinte, G.; Squillaci, M.A.; Ersen, O.; Casiraghi, C.; Ciesielski, A.; Samorì, P. Enhancing the Liquid-Phase Exfoliation of Graphene in Organic Solvents upon Addition of n-Octylbenzene. *Sci. Rep.* **2015**, *5*, 16684. [CrossRef] [PubMed]
23. Haar, S.; Ciesielski, A.; Clough, J.; Yang, H.; Mazzaro, R.; Richard, F.; Conti, S.; Merstorf, N.; Cecchini, M.; Morandi, V.; et al. A supramolecular strategy to leverage the liquid-phase exfoliation of graphene in the presence of surfactants: Unraveling the role of the length of fatty acids. *Small* **2015**, *11*, 1691–1702. [CrossRef] [PubMed]
24. Haar, S.; Bruna, M.; Lian, J.X.; Tomarchio, F.; Olivier, Y.; Mazzaro, R.; Morandi, V.; Moran, J.; Ferrari, A.C.; Beljonne, D.; et al. Liquid-Phase Exfoliation of Graphite into Single- and Few-Layer Graphene with α-Functionalized Alkanes. *J. Phys. Chem. Lett.* **2016**, *7*, 2714–2721. [CrossRef] [PubMed]
25. Díez-Pascual, A.M.; Vallés, C.; Mateos, R.; Vera-López, S.; Kinloch, I.A.; Andrés, M.P.S. Influence of surfactants of different nature and chain length on the morphology, thermal stability and sheet resistance of graphene. *Soft Matter* **2018**, *14*, 6013–6023. [CrossRef]
26. Miranda, P.B.; Pflumio, V.; Saijo, H.; Shen, Y.R. Chain−Chain Interaction between Surfactant Monolayers and Alkanes or Alcohols at Solid/Liquid Interfaces. *J. Am. Chem. Soc.* **1998**, *120*, 12092–12099. [CrossRef]
27. Liang, Y.; Wu, D.; Feng, X.; Müllen, K. Dispersion of Graphene Sheets in Organic Solvent Supported by Ionic Interactions. *Adv. Mater.* **2009**, *21*, 1679–1683. [CrossRef]
28. Parviz, D.; Das, S.; Ahmed, H.S.T.; Irin, F.; Bhattacharia, S.; Green, M.J. Dispersions of Non-Covalently Functionalized Graphene with Minimal Stabilizer. *ACS Nano.* **2012**, *6*, 8857–8867. [CrossRef]
29. Bose, S.; Kuila, T.; Mishra, A.K.; Kim, N.H.; Lee, J.H. Preparation of non-covalently functionalized graphene using 9-anthracene carboxylic acid. *Nanotechnology* **2011**, *22*, 405603. [CrossRef]
30. Su, Q.; Pang, S.; Alijani, V.; Li, C.; Feng, X.; Müllen, K. Composites of Graphene with Large Aromatic Molecules. *Adv. Mater.* **2009**, *21*, 3191. [CrossRef]
31. Ghosh, A.; Rao, K.V.; George, S.J.; Rao, C.N.R. Noncovalent Functionalization, Exfoliation, and Solubilization of Graphene in Water by Employing a Fluorescent Coronene Carboxylate. *Chem. Eur. J.* **2010**, *16*, 2700. [CrossRef]
32. Bourlinos, A.B.; Georgakilas, V.; Zboril, R.; Steriotis, T.A.; Stubos, A.K.; Trapalis, C. Aqueous-phase exfoliation of graphite in the presence of polyvinylpyrrolidone for the production of water-soluble graphenes. *Solid State Commun.* **2009**, *149*, 2172. [CrossRef]
33. Skaltsas, T.; Karousis, N.; Yan, H.J.; Wang, C.R.; Pispas, S.; Tagmatarchis, N. Graphene exfoliation in organic solvents and switching solubility in aqueous media with the aid of amphiphilic block copolymers. *J. Mater. Chem.* **2012**, *22*, 21507–21512. [CrossRef]
34. Xu, J.; Dang, D.K.; Tran, V.T.; Liu, X.; Chung, J.S.; Hur, S.H.; Choi, W.M.; Kim, E.J.; Kohl, P.A. Liquid-phase exfoliation of graphene in organic solvents with addition of naphthalene. *J. Colloid. Interface Sci.* **2014**, *418*, 37–42. [CrossRef] [PubMed]
35. Narayan, R.; Lim, J.; Jeon, T.; Li, D.J.; Kim, S.O. Perylene tetracarboxylate surfactant assisted liquid phase exfoliation of graphite into graphene nanosheets with facile re-dispersibility in aqueous/organic polar solvents. *Carbon* **2017**, *119*, 555–568. [CrossRef]
36. Imani, R.; Shao, W.; Emami, S.H.; Faghihi, S.; Prakash, S. Improved dispersibility of nano-graphene oxide by amphiphilic polymer coatings for biomedical applications. *RSC Adv.* **2016**, *6*, 77818–77829. [CrossRef]

37. Dai, Z.Q.; Zhang, W.W.; Zhang, Z.Y.; Wei, B.M.; Yang, Y.K. Cuprous-Catalyzed Cross-Coupling Reaction of Grignard Reagents with Alkyl Halides. *Asian J. Chem.* **2011**, *23*, 4087–4089.
38. Huang, W.Y.; Gao, W.; Kwei, T.K.; Okamoto, Y. Synthesis and Characterization of Poly(alkyl-substituted p-phenylene ethynylene)s. *Macromolecules* **2001**, *34*, 1570–1578.
39. Castro Neto, A.H.; Guinea, F.; Peres, N.M.R.; Novoselov, K.S.; Geim, A.K. The electronic properties of graphene. *Rev. Mod. Phys.* **2009**, *81*, 109. [CrossRef]
40. Ferrari, A.C.; Meyer, J.C.; Scardaci, V.; Casiraghi, C.; Lazzeri, M.; Mauri, F.; Piscanec, S.; Jiang, D.; Novoselov, K.S.; Roth, S.; et al. Raman Spectrum of Graphene and Graphene Layers. *Phys. Rev. Lett.* **2006**, *97*, 187401. [CrossRef]
41. Eckmann, A.; Felten, A.; Mishchenko, A.; Britnell, L.; Krupke, R.; Novoselov, K.S.; Casiraghi, C. Probing the Nature of Defects in Graphene by Raman Spectroscopy. *Nano. Lett.* **2012**, *12*, 3925–3930. [CrossRef]